Integration of Direct Contact Membrane Distillation and Solar Thermal Systems for Production of Purified Water: Dynamic Simulation

A. Remlaoui(✉) and D. Nehari

Smart Structure Laboratory, University Center of Ain-Témouchent, Ain-Témouchent, Algeria
donremlaoui@gmail.com, nehari2746@gmail.com

Abstract. This paper investigates the integration of solar thermal (FPC) energy powering direct contact membrane desalination (DCMD) to produce clean water. The carried out system is modelized and simulated by using the commercial code TRNSYS. Doing this was possible by including a novel component able to simulate the physical behaviour of the DCMD. The simulation of the solar distillation system has been done during the 21st June under the meteorological conditions of Ain Témouchent city (Algeria). The results showed that the present model has a good agreement with the experimental data of the literature. The present desalination system allows getting a daily distillate production around 56 l/d. Furthermore, concerning the performance parameters, it was found that the energy collected, energy delivered by solar coil and to load reach to 953,25 $kJ.h^{-1}$, 929,43 $kJ.h^{-1}$ and 7542 $kJ.h^{-1}$ respectively. The solar fraction ranged from 0 to1 and the collector efficiencies was assessed 36%.

Keywords: Solar desalination · Direct contact membrane distillation · Flat plate collector · TRNSYS · Solar fraction

1 Introduction

Southern Mediterranean countries are facing a growing water scarcity. There are opportunities to address the problem of water scarcity in rural and remote areas through sustainable saltwater desalination technologies. According to the little scale seawater desalination, the membrane distillation (MD) can be a great option especially in view of the possibility to use the solar thermal and low-grade heat directly as the primary source of energy [1, 2]. Membrane Distillation is a half process that consolidates both thermal and membrane process. The Membrane has a direct contact with a seawater on the feed side and a fluid or vaporous stage on the permeate side. Therefore, can be characterized as a procedure for expelling water vapor from aqueous feed solution heated to a temperature under 100 °C. The transfer force of the process is the difference in partial pressures between two sides of the membrane, which causes evaporation on the feed side [1–4]. The present work focuses on using TRNSYS to analyze a combination of solar energy used to produce simultaneously thermal energy for heating

M. Hatti (Ed.): ICAIRES 2019, LNNS 102, pp. 164–172, 2020.
https://doi.org/10.1007/978-3-030-37207-1_17

seawater and electrical energy for desalinate seawater by FPC and DCMD (Direct Contact Membrane Distillation) for SW (seawater) desalination.

2 System Description

The proposed model for freshwater production from brackish water and thermal energy is a combination of direct Contact Membrane Distillation (DCMD) and flat plate solar collector (FPC) as shown in Fig. 1(a). The basic components like solar collector, storage tank, pumps, controller, heat exchanger, DCMD module.

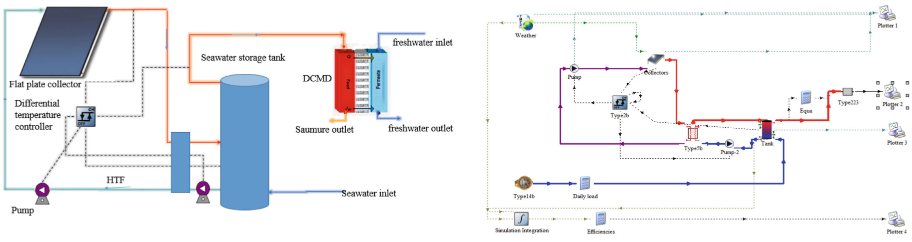

(a) (b)

Fig. 1. (a)Schematic diagram of the FPC-DCMD system and (b) Solar thermal and DCMD systems modeled in TRNSYS 17.

3 TRNSYS Simulation Model

The system described in the previous section was dynamically simulated by transient systems simulation (TRNSYS 17) [5]. Every component model is subroutines ("Type") that exists in the standard library of TRNSYS. TRNSYS software is utilized for analyzing the performance of the system, as the whole system is modeled as shown in Fig. 1(b). Table 1 demonstrates the devices and the corresponding simulation subroutine (Type). Once all the components of the system have been identified and a mathematical description of each component is available, the main components of this model are described and shown in Table 1.

3.1 Solar Collectors and Thermal Storage

Solar thermal collector is simulated using type 1b model. The following equations are the basic equations for the useful collector energy Q_u (kJ.h^{-1}) [6, 7] and for the collector efficiency η_{coll} [8, 9]:

$$Q_u = \dot{m}_{fs} C_{p,fs} (T_{outcol} - T_{incol}) \tag{1}$$

$$\eta_{coll} = \frac{Q_u}{A_c G_T} = \eta_0 - a_1 \frac{(T_{av} - T_{amb})}{G_T} - a_2 \frac{(T_{av} - T_{amb})^2}{G_T} \tag{2}$$

Table 1. The components and input design parameters in Transys17 simulation programs

Component	Type	Input parameter	Value
Flat plate solar thermal collector	TYPE 1b	Number in series Collector absorber area (m^2) Fluid specific heat (kj/kgk) Tested flow rate (kg/h) Intercept efficiency First order efficiency coefficient (kj/hm^2k) Second order efficiency coefficient (kj/hm^2k^2)	2 5 3.708 40 0.8 13 0.05
Pump	TYPE 3b	Rated flow rate (kg/h) Rated power (kj/h)	200 240
Heat exchanger	TYPE 5b	Specific heat of hot side fluid (kj/kgk) Specific heat of cold side fluid (kj/kgk)	3.708 4.19
DCMD	TYPE 223	Membrane material Membrane length (m) Pore size (µm) Contact angle (Degrees) Membrane area (m^2) Membrane Width (m) Specific heat of freshwater ($J.kg^{-1}\ K^{-1}$) Specific heat of feedwater ($J.kg^{-1}\ K^{-1}$) Feed water speed ($m.s^{-1}$) Salinity ($g_{NaCl}.L^{-1}_{water}$)	PTFE 0.145 1 126 0,0136 0.1 4190 4190 0.4 10
Thermal storage tank	TYPE 4c	Tank volume (m^3) Fluid specific heat ($kJ\ kg^{-1}\ K^{-1}$) Fluid density ($kg\ m^{-3}$) Tank loss coefficient ($Wm^{-2}\ K^{-1}$) Set point temperature for element (C) Dead band for heating element 1 (C) Maximum heating rate of element 1 ($kJ\ h^{-1}$)	0.3 4.19 1000 0.6944 60 5 9000
Weather data reading and processing Mains seawater supply profile Online plotter Integrator Controller	TYPE1 5-6TM2 TYPE 14 h TYPE 65c TYPE 24 TYPE 2b	Ain Temouchent Flow rate (kg/h)	

Where T_{incol} and T_{outcol} are the inlet and outlet temperature of the solar fluid (K),$\dot{m}_{fs}$ is the solar fluid mass flow rate ($kg.h^{-1}$) and $C_{p,fs}$ is the specific heat capacity of solar fluid ($kJ.kg^{-1}\ K^{-1}$), G_T is the incident total solar radiation ($kJ.h^{-1}.m^{-2}$), A_c is the collector gross area (m^2), η_0 is the optical efficiency,a_1 is the global heat loss coefficient ($kJ.h^{-1}.m^{-2}.K^{-1}$) and a_2 is the temperature dependence of the global heat loss coefficient ($kJ.h^{-1}.m^{-2}.K^{-2}$);T_{amb} Ambient temperature. The thermal storage tank is subjected to thermal stratification and modeled using type 4c.

3.2 Heat Exchanger and Membrane Distillation

Counter flow heat exchanger of Type 91 is used in the model. The simulation run using TRNSYS17 software has been executed via injected a new-programed component; in particular, TYPE 223 is added to the standard library. This new TYPE is committed to a desalination unit DCMD. This component is written by FORTRAN language. The membrane distillation process is governed by different heat and mass transfer mechanisms that occur at both the feed side, the membrane and the permeate side. Mass transfer occurs through the pores of the membrane while heat is transferred through both the membrane and its pores. The mass flux J_w ($L/(m^2.h)$) of water can be written as a linear function of the vapor pressure difference (P_{mf} and P_{mp} as a function of the temperature on the feed (T_{mf}) and permeate (T_{mp}) at the membrane surface (C)) across the membrane and the membrane mass transfer coefficient B_m ($L/(m^2h.Pa)$) [10], given by:

$$J_w = B_m\left(P_{mf} - P_{mp}\right) \tag{3}$$

The heat transfer involved in DCMD the heat flux can be written as follows [9, 11]:

$$Q = \left(\frac{1}{h_f} + \frac{1}{h_m + \frac{j_w \Delta H_v}{T_{mf} - T_{mp}}} + \frac{1}{h_p}\right)^{-1}\left(T_{bf} - T_{bp}\right) \tag{4}$$

4 The Energy Performance Indices

The energy performance indices evaluated in this study include: energy collected (Q_u), energy delivered by solar coil (Q_d) and delivered to load (Q_{load}), auxiliary energy (Q_{aux}), solar fraction (SF), collector efficiency (η_{coll}) and system efficiency (η_{sys}). The useful energy delivered by the solar coil to the hot water tank is given as:

$$Q_d = \dot{m}_{fs} C_{p,fs}\left(T_{outcoil} - T_{incoil}\right) \tag{5}$$

Where T_{incoil} solar fluid temperature at inlet to the solar coil, $T_{outcoil}$ solar fluid temperature at the outlet from the solar coil (°C).

4.1 Solar Fraction (SF)

Ratio of net utilized solar energy for SSH to total SSH demand including auxiliary energy [6, 7] is in this way:

$$SF = \frac{Q_d}{Q_d + Q_{aux}} \tag{6}$$

4.2 System Efficiency (η_{sys})

The efficiency of the FPC system is calculated as:

$$\eta_{sys} = \frac{Q_d}{A_c G_T} \tag{7}$$

5 Results and Discussion

5.1 Validation of the DCMD Model

In order to validate our numerical predictions based on the new TRNSYS component (DCMD unit); we have studied the system designed by Jianhua Zhang [11]. Figure 2 shows the comparison between the given experimental results [8] and the numerical results obtained from the model used in the present investigation. It can be noticed that the permeate flux predicted by the present model has a good agreement with the experimental data.

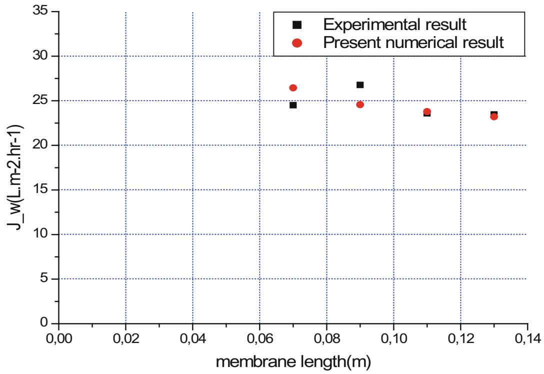

Fig. 2. Validation of the numerical model at (Tcin = 20 °C, Thin = 60 °C, V = 0.4 m.s^{-1}) with Jianhua Zhang [11] experimental result.

5.2 FPC Outlet Temperature

Figure 3(a) shows the plots of the solar fluid temperature in the outlet of FPC. It is seen that the modelled values follow has reached the uttermost value of 140 °C at the outlet of FPC in the tested days.

5.3 Hot Water Outlet Temperature

Figure 3(b) shows the hot water tank outlet fluid temperature for the FPC system measured along the hot water discharge pipe. The peaks show the outlet fluid temperatures during water draw-offs. It is seen that during the clear sky day the tank outlet fluid temperature stayed above 60 °C since energy was added to its content throughout the day thereby raising its temperature.

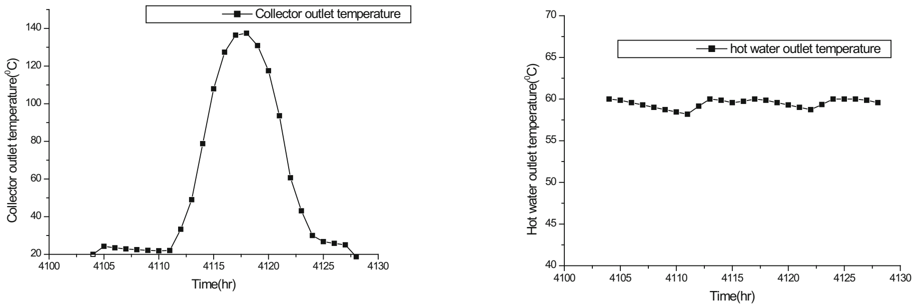

(a) (b)

Fig. 3. Modelled (a) collector outlet temperature and (b) hot seawater outlet temperature for FPC system

5.4 The Permeate Flow of the DCMD System

The Fig. 4(a) presents the total mass transfer of the membrane during a summer day (June 21st). At feed side, the seawater inlet temperature is in the range 60–79.22 °C (not shown here), at permeate side, freshwater inlet temperature was about 25 °C and. The maximum production flux of the permeate is 12 L.h^{-1}.

5.5 Energy Collected (Q_u)

Figure 4(b) illustrates the energy supplied by the solar collector (Qu) that is provided to HTF for each hour during 21st June. The results of the simulation indicate during the time interval 8 am to 6 pm that the energy supplied by the solar collector is between 35,47 kJ.h^{-1} and 953,25 kJ.h^{-1}.

5.6 Energy Delivered by Solar Coil (Q_d) and Delivered to Load (Q_{load})

Figure 5(a) shows the total heat transfer rate across heat exchanger Q_d and energy delivered to load Q_{load} for each hour during 21 June. It can be seen in Fig. 5(a) hat the

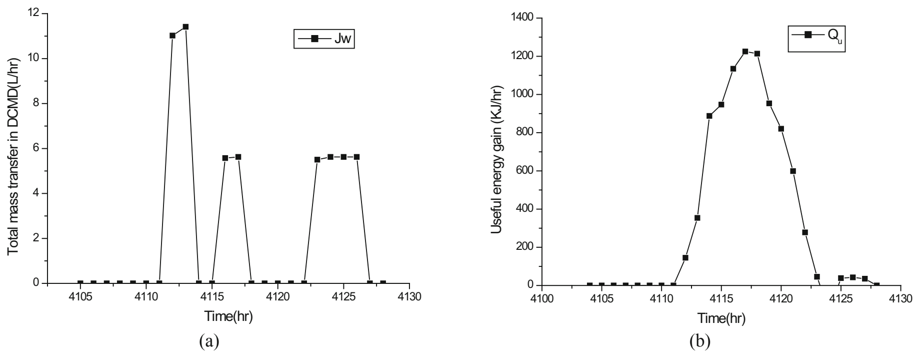

Fig. 4. Modelled (a) permeate flow of the DCMD system and (b) energy collected by FPC collector.

total heat transfer rate across heat exchanger Q_d is ranged between 72,59 kJ.h^{-1} and 929,43 kJ.h^{-1}, this parameter is proportionally to the solar radiation variation. In addition, in the first half daylight between 8 am to 14 pm (4110 h to 4116 h), the Q_d increasing until reach a hight value and this due to the rise of Qu of solar fluid. Whereas, for the second half daylight from the time 4117 h, the Q_d decreases due to diminution of solar radiation and Qu. It is seen in Fig. 5(a) that the FPC system delivered to load is ranged between 3771 kJ.h^{-1} and 7542 kJ.h^{-1}.

5.7 Auxiliary Energy (Q_{aux})

The results of the simulation indicate during the time interval 8 am to 6 pm that the auxiliary heating consumed a highest value of 3859.88 kJ.h^{-1} at the time 4113 h. This means that the high value of the solar radiation leads to minify the intervention of the auxiliary heater to augment the brackish water temperature until 60 °C.

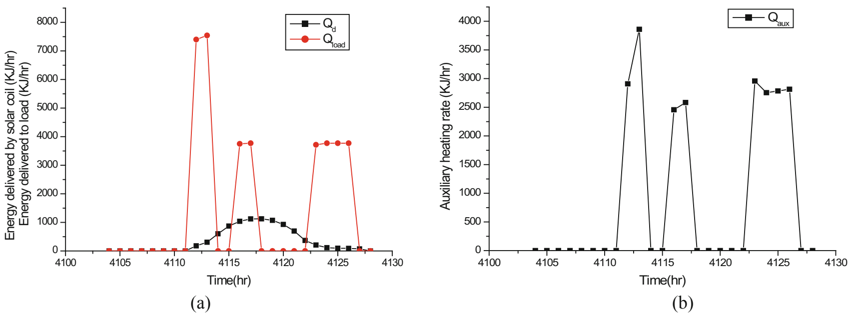

Fig. 5. Modelled (a) the total heat transfer rate across heat exchanger and energy delivered to load and (b) auxiliary energy in 21st June

5.8 Solar Fraction (SF)

According to the Fig. 6(a), the solar fraction SF for the FPC systems is presented. The SF is in the range $0 \leq SF \leq 1$, the solar savings fraction get zero ‘0’ value for no solar energy utilization, and have the value 1 when the energy is provided only via solar way. For intermediate values different from 0 and 1, the pump and auxiliary heater work together.

5.9 Collector Efficiency (η_{coll}) and System Efficiency (η_{sys})

Concerning solar collector thermal efficiency η_{coll}, its maximum value in our case is 0.36 (i.e. 36%). This value is related to one collector with area of 1 m^2. The FPC system efficiency η_{sys} is also confined between 0.23 and 0.35

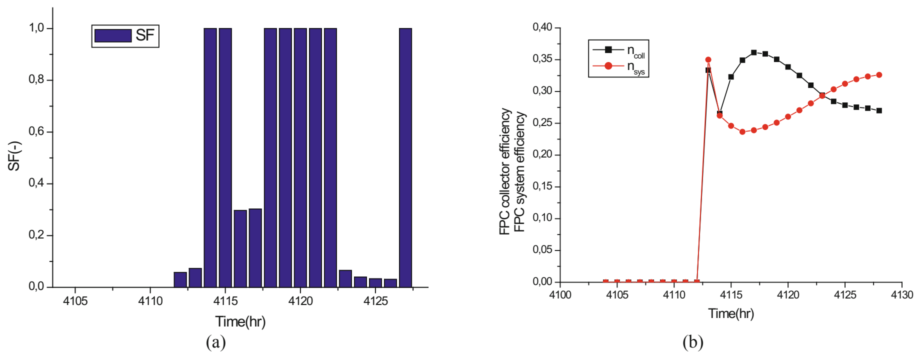

Fig. 6. Modelled (a) Solar fraction and (b) solar collector thermal efficiency and FPC system efficiency for n = 1FPC and S = 1 m^2

6 Conclusion

In this study, a new type of solar-energy-integrated DCMD system for seawater desalination was tested under actual environmental conditions in Ain Témouchent, Algeria. The system was simulated using TRNSYS program. A new TRNSYS component type of DCMD system has been built and added in TRNSYS library as type 223. The type was been included in the scheme with other additional components required for the solar desalination system. The simulation during the 21st June as a typical day in order to evaluate the thermal behaviors of the desalination system. The proposed solar DCMD system has shown favorable potential application in desalination of seawater. The HTF temperatures reached the highest value of 140 °C at the outlet of FPC. Solar thermal driven DCMD system can produce 12 kg/h in June 21st of drinking water. A TRNSYS simulation result was showed that the system was able to generated between 35,47 $kJ.h^{-1}$ and 953,25 $kJ.h^{-1}$ of heat whereas the auxiliary heating consumed a highest value of 3859,88 $kJ.h^{-1}$ to augment the seawater temperature from the 60 °C. The total heat transfer rate across the heat exchanger ranges between 72,59 $kJ.h^{-1}$ and 929,43 $kJ.h^{-1}$. The performance parameters, which are the solar fractions, ranged from 0 to1 and the collector efficiencies was assessed 36%.

References

1. Schwantes, R., Cipollina, A., Gross, F., Koschikowski, J., Pfeifle, D., Rolletschek, M., Subiela, V.: Membrane distillation: solar and waste heat driven demonstration plants for desalination. Desalination **323**, 93–106 (2013)
2. Khayet, M.: Solar desalination by membrane distillation: dispersion in energy consumption analysis and water production costs (a review). Desalination **308**, 89–101 (2013)
3. Bahmanyar, A., Asghari, M., Khoobi, N.: Numerical simulation and theoretical study on simultaneously effects of operating parameters in direct contact membrane distillation. Chem. Eng. Process. **61**, 42–50 (2012)
4. Ashoor, B.B., Mansour, S., Giwa, A., Dufour, V., Hasan, S.W.: Principles and applications of direct contact membrane distillation (DCMD): a comprehensive review. Desalination **398**, 222–246 (2016)
5. TRNSYS: Transient System Simulation tool. http://www.trnsys.com/
6. Vargas-Bautista, J.P., García-Cuéllar, A.J., Pérez-García, S.L., Rivera-Solorio, C.I.: Transient simulation of a solar heating system for a small-scale ethanol-water distillation plant: thermal, environmental and economic performance. Energy Convers. Manag. **134**, 347–360 (2017)
7. Cao, F., Zhao, L., Zhang, F., Guo, L.: Redesign of a water heating system using evacuated tube solar collectors: TRNSYS simulation and techno-economic evaluation. Heat Transf. Eng. **35**, 556–566 (2014)
8. Mohan, G., Kumar, U., Pokhrel, M.K., Martin, A.: A novel solar thermal polygeneration system for sustainable production of cooling, clean water and domestic hot water in United Arab Emirates: Dynamic simulation and economic evaluation. Appl. Energy **167**, 173–188 (2016)
9. Bui, V.A., Vu, L.T.T., Nguyen, M.H.: Modelling the simultaneous heat and mass transfer of direct contact membrane distillation in hollow fibre modules. J. Membr. Sci. **353**, 85–89 (2010)
10. Eleiwi, F., Ghaffour, N., Alsaadi, A.S., Francis, L., Laleg-Kirati, T.M.: Dynamic modeling and experimental validation for direct contact membrane distillation (DCMD) process. Desalination **384**, 1–11 (2016)
11. Zhang, J., Li, J.-D., Gray, S.: Researching and modelling the dependence of MD flux on membrane dimension for scale-up purpose. Desalination Water Treat. **31**, 144–150 (2011)